Optical Phonons in Nanoclusters Formed by the Langmuir-Blodgett Technique

A. Milekhin,[1,2,*] L. Sveshnikova,[1] T. Duda,[1]
N. Surovtsev,[3] S. Adichtchev,[3] and D. R. T. Zahn[4]

[1]*Institute of Semiconductor Physics, Novosibirsk, Russia*
[2]*Novosibirsk State University, Novosibirsk, Russia*
[3]*Institute of Automation and Electrometry, Novosibirsk, Russia*
[4]*Semiconductor Physics, Chemnitz University of Technology, Chemnitz, Germany*

(Received April 12, 2010)

The spectrum of optical phonons (including localized transverse and longitudinal optical phonons, as well as their overtones and surface optical phonons) in semiconductor CdS, PbS, ZnS, ZnO, CuS, and Ag2S nanocrystals formed by the Langmuir-Blodgett technique on solid substrates is studied using non-resonant, resonant, and surface-enhanced Raman as well as Infrared spectroscopies.

PACS numbers: 78.30.-j; 78.67.Hc

I. INTRODUCTION

II-VI and IV-VI nanocrystals (NCs) have been extensively studied due to their attractive optical, electronic, and magnetic properties resulting in a number of applications, especially in nonlinear optics, optoelectronics, and biology [1–5]. A number of experimental techniques such as colloid and wet chemistry [4, 6, 7], formation in glasses [4], epitaxial growth [5], ion implantation and lithography techniques [5], etc. is used for the formation of semiconductor NCs. Among those, the Langmuir-Blodgett (LB) technology is considered as a low-cost and flexible method for the fabrication of various II-VI and IV-VI NCs.

Raman spectroscopy is traditionally applied for the identification of NCs distributed in various matrices and for the determination of their crystal structure [3]. Complementary to Raman scattering and due to different selection rules, IR spectroscopy provides additional information on the lattice vibrations of NCs. Cadmium chalcogenide NCs belong to the most investigated system the vibrational spectrum of which was studied in detail both theoretically and experimentally [8–11]. However, today's science technology and semiconductor industry require cadmium-free, non-toxic nanocrystal materials with superior optical properties.

Here we present a comparative study of vibrational properties of CdS and cadmium-free NCs formed using LB technology.

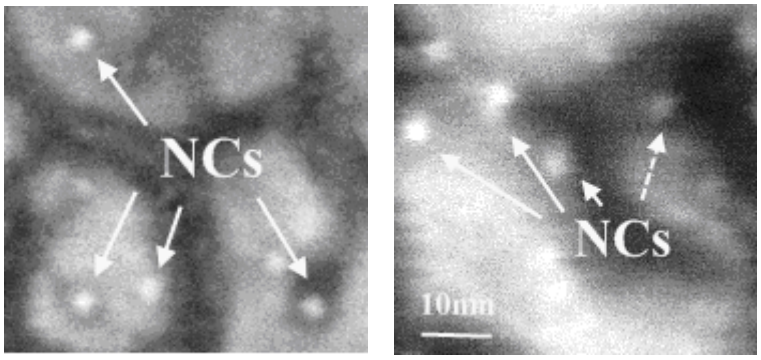

FIG. 1: SEM images of free-standing CdS NCs formed after annealing of LB film with thicknesses of a) 2 and b) 4 MLs. The position of CdS NCs is indicated by arrows. The non-homogeneous background is due to the island growth of Au on Si. The height of the islands is typically about 4 nm.

II. EXPERIMENT

High quality films of Cd, Zn, Pb, Cu and Ag behenates were prepared using the LB technology on (001)-oriented Si substrates covered by a 100 nm thick Au layer. The thickness of the LB films under investigation was varied in the range from 2 to 440 monolayers (MLs). The reaction of the behenates with gaseous H_2S results in the formation of CdS, ZnS, PbS, CuS, and Ag_2S NCs. Free standing NCs were obtained after removing the organic matrix by thermal annealing in an inert atmosphere at temperatures between 100 and 250°C. Free standing ZnO NCs were formed as a result of annealing of either Zn behenate films or ZnS NCs at 600°C in air.

Raman scattering experiments were carried out using a Dilor XY800 spectrometer in backscattering geometry at 40 and 300 K. Kr^+, Ar^+ ion, and HeCd lasers were used as excitation sources in the wavelength range from 752.5 to 441 nm.

IR reflection spectra were recorded at grazing incidence (angle of incidence is $\theta \approx 80°$) using an IR Fourier transform spectrometer Vertex 80v in the spectral range of the optical vibrations ($50 \div 700$ cm^{-1}) of the crystal lattices in the chalcogenides. IR spectra were taken at room temperature using non-polarized light.

III. DISCUSSION

The structural properties of the NCs were studied by scanning electron microscopy (SEM). Typical SEM images of CdS NCs with different areal densities are shown in Fig. 1. The size of CdS NCs determined from the SEM images is varied in the range from 2 to 5 nm. The size of NCs of all materials under investigation does not exceed the value of 10 nm.

According to X-ray diffraction measurements PbS and ZnS NCs have predominantly

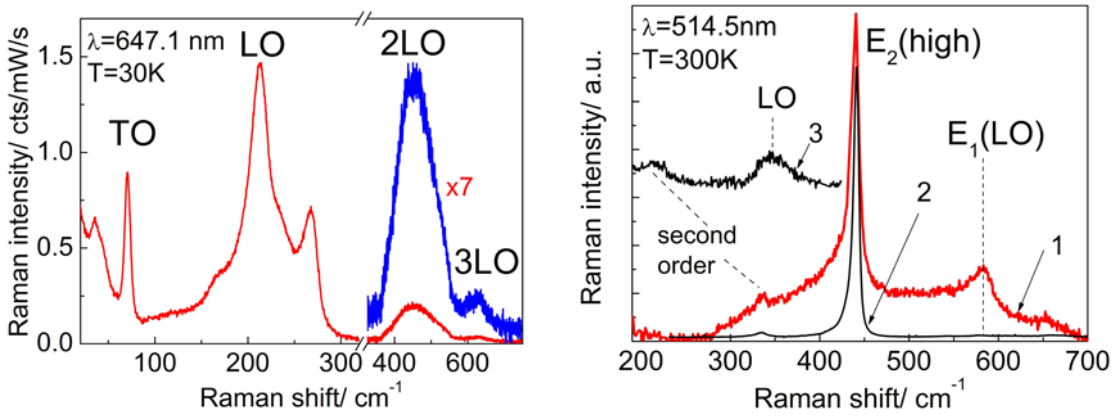

FIG. 2: Raman spectra of a) PbS and b) curve 1- ZnO NCs, curve 2- (0001) ZnO crystal, curve 3- ZnS NCs.

cubic structure, CdS and ZnO NCs are hexagonal, while Ag_2S NCs reveal monoclinic symmetry. A variety of crystal modifications of CuS with similar lattice parameters complicates the analysis of crystal structure of the CuS NCs. A detailed analysis of XRD results will be published elsewhere.

The Raman spectra of NCs were recorded in the spectral range of the lattice vibrations of materials composing the NCs. Fig. 2(a) shows the Raman spectrum of PbS NCs formed from a LB film with a thickness of 400 MLs. Note, that the Raman spectra of PbS NCs were measured in resonance with the energy of interband transitions in the NCs derived from absorption spectra (not shown here). The interband transition energy of PbS NCs amounts to about 2.1 eV. It is shifted towards higher energies with respect to the band gap of bulk PbS (0.4 eV) due to the confinement effect. The peaks at about 70 cm^{-1} and the features at 174 and 270 cm^{-1} seen in the Raman spectrum of PbS NCs (Fig. 2(a)) are assigned to the TO phonons and to 2TO phonon along $\Sigma(2 \times 135 = 270)$ cm^{-1} of the PbS NC phonons, respectively, according to the conclusions made for bulk PbS in [12, 13]. The peaks at 212, 430, and 636 cm^{-1} correspond to the scattering by LO(Γ) phonons localized in NCs and their overtones (2LO and 3LO), respectively, confirming a high crystalline quality of the NCs.

The Raman spectrum of free-standing ZnO NCs was measured at the non-resonant conditions (Fig. 2(b)). For comparison the Raman spectrum of wurtzite ZnO crystal was measured in the same experimental conditions with the incident light parallel to c-axis of ZnO crystal. The spectra of ZnO bulk crystal and ZnO NCs reveal an intensive peak at 440 cm^{-1} which is attributed to the E_2 phonon mode. The weaker peak at about 335 cm^1 seen in both spectra is attributed to second-order Raman processes [14]. The mode at 584 cm^{-1} seen in the Raman spectrum of ZnO NCs (Fig. 2(b)) is still under debate. This mode is observed in the Raman spectra of both ZnO bulk and NCs (with higher intensity) and, therefore, can be attributed to E_1(LO) phonons [15]. The enhanced intensity of the mode can manifest the weakening of selection rules in ZnO NCs with respect to the bulk

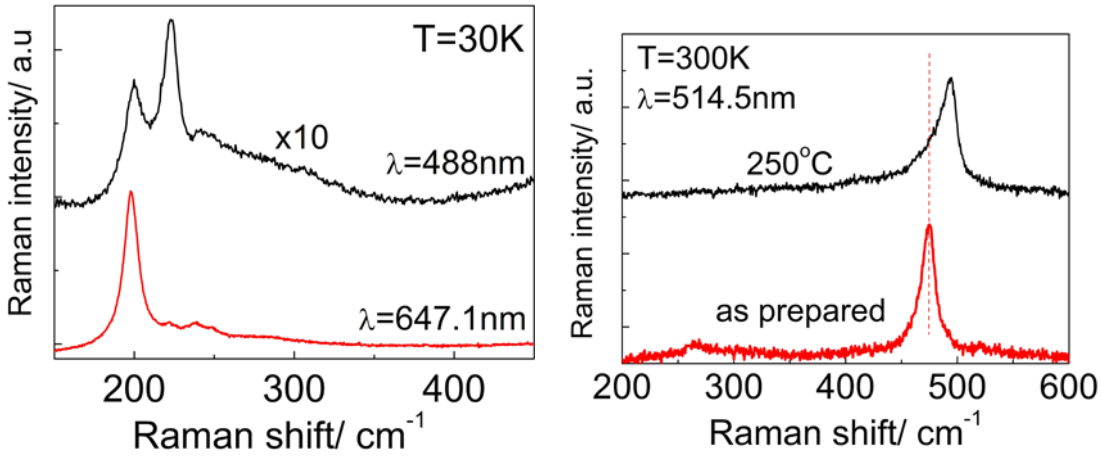

FIG. 3: Raman spectra of a) Ag_2S NCs measured in resonant (λ = 647.1 nm) and non-resonant conditions (λ = 488 nm) and b) as-prepared CuS NCs and the NCs annealed at 250°C.

material. On the other hand, a mode with the same frequency position assigned to confined LO phonons is expected in ZnO NCs according to theoretical calculations [16].

The Raman spectrum of free-standing ZnS NCs (Fig. 2(b)) shows a broad peak at 347 cm^{-1} attributed to LO phonons in the NCs and a weaker feature at 211 cm^{-1} due to second order Raman scattering (TO(X)-TA(X)) [17]. The frequency position of the LO mode is shifted towards lower frequencies with respect to the corresponding value in cubic ZnS (351 cm^{-1}). This can be due to the confinement effect of optical phonons in the NCs.

Raman spectra of Ag_2S NCs (Fig. 3(a)) measured at low temperature (30K) demonstrate a strong resonance dependence. In the non-resonant conditions (λ_L below 600 nm) two intensive features at 200 and 222 cm^{-1} are observed. At the resonant conditions (at 647.1 nm) the intensity of the mode at 200 cm^{-1} is increased by a factor of 10 while the mode at 222 cm^{-1} is vanishing. It was already reported that the Raman spectra of Ag_2S thin films measured with λ_L = 514.5 nm at room temperature show one very broad band (centered around 220 cm^{-1}) which may be an indication of an amorphous material [18]. The observation of Raman scattering by the lattice vibrations in monoclinic Ag_2S at about 200 and 220 cm^{-1} and their identification as Ag and Bg, respectively, using a charge-dipole molecular dynamical calculation were reported in a detailed spectroscopic study of bulk Ag_2S [20].

Much less is known about the vibrational spectrum of CuS NCs.

The Raman scattering by phonons in CuS NCs reveals no resonance behavior. This is in accordance with the featureless absorption spectrum of CuS NCs. Raman spectra of as-prepared CuS NCs embedded in the LB film are shown in Fig. 3(b). The spectra reveal an intensive peak at 474 cm^{-1} and a weaker feature at 265 cm^{-1} (at T=300K) which are assigned to lattice vibrations in CuS NCs. These data coincide with earlier results [18, 19] for CuS thin lms. It is worth mentioning, that the spectra remain almost the same after

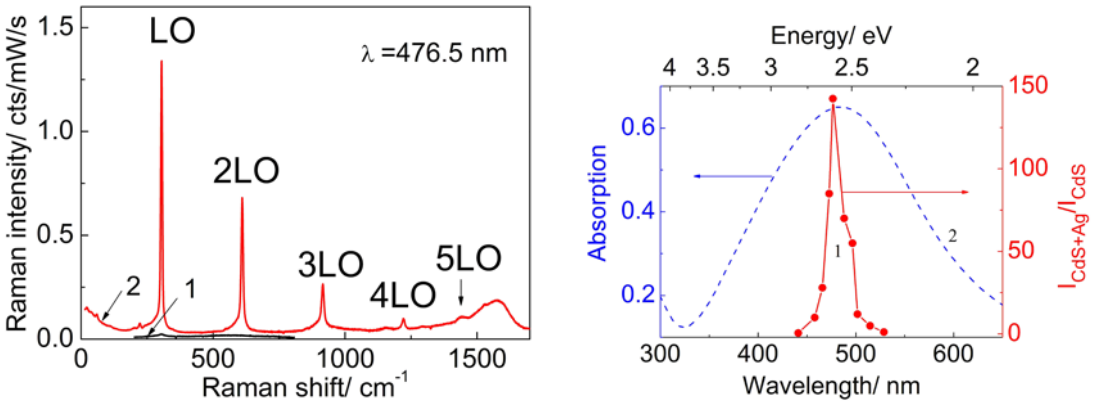

FIG. 4: a) Raman (curve 1) and SERS (curve 2) spectra of CdS NCs measured with $\lambda = 476.5$ nm. b) The resonant profile and the absorption spectrum of Ag nanocrystals.

annealing to 150°C while annealing at higher temperatures leads to the appearance of a new peak at about 490 cm^{-1}. The origin of this feature is not established and requires further investigation. However, the symmetry analysis of the lattice vibrations in CuS has not been performed yet.

The Raman scattering by phonons in the arrays of CdS NCs is well established and understood. It reveals a dominant feature at 300 cm^{-1} attributed to LO phonons in the NCs [2, 4, 8–11]. Recently, it was reported that the deposition of silver on CdS NCs causes a significant enhancement of the Raman intensity of LO phonons manifesting the existence of surface-enhanced Raman scattering [21]. Fig. 4(a) shows Raman spectra of free-standing CdS NCs formed after annealing of the corresponding LB film with a thickness of 440 MLs before and after Ag deposition measured at 30K. It is clearly seen that the intensity of the LO mode is drastically increased and new modes attributed to its overtones up to fourth order (2LO-5LO) are observed. The low frequency shoulder of nLO modes can also be seen in the spectra. The shoulder is due to surface optical (SO) phonons and their overtones (nSO). A broad feature near 1600 cm^{-1} can be attributed to SERS either from amorphous carbon species [22] or from Ag_2O [23]. The resonance profile, i.e. the ratio of Raman intensities of the mode after and before Ag deposition as a function of the laser excitation energy, presented in Fig. 4(b) reveals a maximum of the SERS enhancement which amounts to about 140. The energy of the maximum corresponds to the energy of the localized plasmon in Ag nanoclusters which makes surface-enhanced Raman scattering possible.

It has been already established that the distance between metal nanoclusters and a SERS active medium is crucial for the Raman enhancement [24]. The first few nanometers of the active medium give a dominant contribution to the SERS enhancement. Therefore, it is expected that the lower lying NCs give a minor contribution to the SERS enhancement. Indeed, decreasing of the nominal thickness of CdS NC layers from 440 to 30 MLs (factor of about 14.7) exhibits only three-fold decrease of the SERS intensity by LO phonons. This

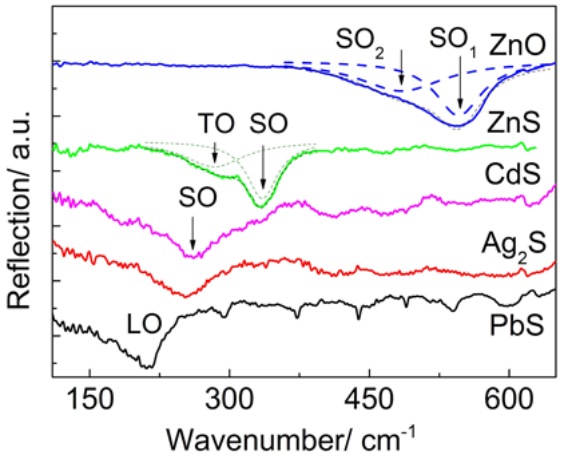

FIG. 5: IR spectra of NCs measured at oblique incidence ($\theta \approx 75°$) using non-polarized light at a temperature of 300K. The results of fitting with Lorentzian line shapes are shown by dashed lines.

corresponds to 700-fold SERS enhancement of the Raman intensity of LO phonons and opens perspectives for studying the NC arrays of very low areal densities.

The IR reflection-absorption spectra of free standing CdS, ZnS, PbS, Ag_2S, and ZnO NCs are presented in Fig. 5.

The IR spectrum of ZnO NCs demonstrates the most intensive absorption. Obviously, this absorption band consists of two lines (indicated as SO_1 and SO_2 which are centered at 546 and 484 cm^{-1}, respectively) distinguished by curve fitting. Their frequency positions are situated between the LO and TO phonon frequencies of the IR-active E_1 and A_1 vibrational modes, respectively. According to calculation of the phonon spectrum of spherical ZnO NCs [16] and the literature Raman data [25] these modes can be attributed to surface optical phonons. The frequency positions of the SO phonons (548 and 490 cm^{-1}) are consistent with those calculated within the dielectric continuum model [26] supposing a spherical shape of NCs. In the calculations, the dielectric constants obtained earlier for ZnO films [27] were used.

The frequency position of the minimum in the IR spectrum of PbS at about 210 cm^{-1} corresponds well to the LO phonon mode (Fig. 5). A low-frequency shoulder of the minimum can be attributed to the influence of absorption by SO phonons [11]. The IR spectrum of CdS NCs exhibits a broad feature at the frequency range between the TO and LO phonon positions assigned to SO phonons in the free-standing CdS NCs according to our previous observation [11]. The absorption feature seen in the spectra of ZnS NCs consists from two components. The spectra were curve fitted with the Lorentzian line shapes to reveal the individual absorption bands at 330 and 283 cm^{-1} attributed to SO and TO phonons in ZnS NCs, respectively. The frequency position of the SO mode corresponds well with that (332 cm^{-1}) calculated in [28].

As in the case of the analysis of Raman data, the assignment of the broad feature

observed in the IR spectrum of Ag_2S NCs at 250 cm^{-1} is not obvious. The only IR reflection study of monoclinic Ag_2S available in literature [29] shows a broad band due to lattice vibration in the spectral region from 220 to 250 cm^{-1}. Therefore, most probably, this feature can be attributed to IR active lattice vibrations of monoclinic Ag_2S NCs.

IV. CONCLUSIONS

CdS, PbS, ZnS, ZnO, CuS, and Ag_2S nanocrystals embedded in an organic matrix and free-standing on solid substrates are formed by the Langmuir-Blodgett technique. The combination of IR spectroscopy and Raman scattering (including non-resonant, resonant, and surface-enhanced Raman scattering) are employed to probe the vibrational spectrum of NCs. On the basis of the experimental data and the calculations, the spectrum of optical phonons (including localized TO and LO phonons, as well as their overtones and surface optical phonons) for NCs is established. It is shown that surface-enhanced Raman scattering can be effectively applied for studying the phonon spectrum of the NCs with a low areal density.

Acknowledgments

This work was supported by the Russian Foundation for Basic Research (grant 09-02-00458a) by Siberian Branch of the Russian Academy of Sciences (grant SB RAS-Belarus № 9), Deutsche Forschungsgemeinschaft (grant Za146/22-1) and the International Research Training Group (Internationales Graduiertenkolleg, GRK 1215) "Materials and Concepts for Advanced Interconnects". The authors are thankful to Dr. M. Kehr and Dr. S. Kosolobov for XRD and SEM measurements, respectively.

References

* Electronic address: milekhin@thermo.isp.nsc.ru

[1] Gaponenko S. V., *Optical Properties of Semiconductor Nanocrystals*, (Cambridge: Cambridge University Press) 1998.
[2] Bandyopadhyay S. and Nalwa H. S. (Eds), *Quantum dots and Nanowires*, (California: American Scientific Publishers) 2003.
[3] Nalwa H. S. (Ed.), *Nanostructured Materials and Nanotechnology*, (San Diego: Academic Press) 2002.
[4] Woggon U., *Optical properties of Semiconductor Quantum Dots*, (Berlin, Heidelberg: Springer-Verlag) 1997.
[5] D. Bimberg, M. Grundmann, N. N. Ledentsov, *Quantum Dots Heterostructures*, (Chichester, New York, John Wiley & Sons) 1999.
[6] C. B. Murray, D. J. Norris, M. G. Bawendi, J. Am. Chem. Soc. **115** (19), 8706–8715 (1993).
[7] P. V. Kamat and D. Meisel, *Semiconductors Nanoclusters*, (Elsevier, New York, 1996), Vol. 103.

[8] M. I. Vasilevskiy, Phys. Rev. B **66**, 195326 (2002).
[9] A. G. Rolo and M. I. Vasilevskiy, J. Raman Spectrosc. **38**, 618–633 (2007).
[10] A. I. Belogorokhov *et al.*, JETP **104**(1), 111 (2007).
[11] A. G. Milekhin *et al.*,Thin Solid Films **422**, 200–204 (2002).
[12] P. G. Etchegoin *et al.*, Phys. Stat. Sol. (b) **245**(6), 1125 (2008).
[13] A. H. Romero *et al.*, Phys. Rev. B **78**, 224302 (2008).
[14] K. A. Alim *et al.*, J. Appl. Phys. **97**, 124313 (2005).
[15] T. Wermelinger and R. Spolenak, J. Appl. Phys. **106**, 064907 (2009).
[16] V. A. Fonoberov and A. A. Balandin, Phys. Rev. B **70**, 233205 (2004).
[17] J. Serrano *et al.*, Phys. Rev. B **69**, 014301 (2004).
[18] BṀinceva-Sukarova, M. Najdoski, L. Grozdanov, C. J. Chunnilall, J. Mol. Struct. **410** , 267 (1997).
[19] S.-Y. Wang, W. Wang, Z.-H. Lu, Materials Science and Engineering B **103**, 184–188 (2003).
[20] M. Ishii and H. Wada, Mat. Res. Bull. **28**, 1269–1276 (1993).
[21] A. G. Milekhin *et al.*, JETP Lett. **88**(12), 799–801 (2008).
[22] O. L. A. Monti, J. T. Fourkas, and D. J. Nesbitt, J. Phys. Chem. B **108**, 1604–1612 (2004).
[23] C.-M. Chuang, M.-C. Wu, and W.-F. Su, K.-C. Cheng, Y.-F. Chen, Appl. Phys. Lett. **89**, 061912 (2006).
[24] R. Aroca, *Surface-Enhanced Vibrational Spectroscopy*, John Wiley & Sons (The Atrium, Southern Gate, Chichester, West Sussex, England), 2006.
[25] H. F. Liu, S. Tripathy, G. X. Hu, and H. Gong, J. Appl. Phys. **105**, 053507 (2009).
[26] P. A. Knipp, T. L. Reinecke: Phys. Rev. B **46**, 10 310 (1992).
[27] N. Ashkenov *et al.*, J. Appl. Phys. **93**(1) (2003).
[28] J. Xu, H. Mao, Y. Sun, and Y. Du, J. Vac. Sci. Technol. B **15**(4), 1465 (1997).
[29] P. Bruesch, J. Wullschleger, Solid State Comm. **13**, 9 (1973).